Seismicity based reservoir characterization - case studies and numerical verifications of the approach

E. Rothert and S. A. Shapiro

email: *rothert@geophysik.fu-berlin.de*

keywords: *Permeability, hydraulic diffusivity, induced microseismicity, reservoir characterization*

ABSTRACT

The SBRC approach uses microseismicity for reservoir characterization. A geometrical optic like formalism was proposed to describe the kinematics of the propagation of seismicity triggering fronts (Shapiro et al., 2001). This formalism is similar to the eikonal equation for seismic wavefronts and it serves as a base for the inversion of the passive monitoring data for the permeability distribution. Here, the approach is further developed and numerically tested. We show how it can be applied to Hot-Dry-Rock and hydrocarbon reservoirs. We also attempt to model the phenomenon of the triggering process and to test the inversion algorithms numerically. Therefore, methods are developed to create synthetic microseismicity clouds induced by pore pressure perturbations in hydraulically homogeneous and heterogenous media. Excellent agreements are found for theory and observations which emphasize the main process of the triggering phenomenon and the practicability of the reconstruction algorithms.

INTRODUCTION

The SBRC approach is based on the hypothesis that the triggering front of the hydraulic-induced microseismicity propagates like the low-frequency second-type compressional Biot wave corresponding to the process of pore-pressure relaxation (see Shapiro et al, 1997, 1999 and the recent discussion of the method in Cornet 2000 and Shapiro et al, 2000). In realistic fluid injections the dominant frequencies of pore-pressure perturbations are much lower than the critical Biot frequency, which is usually greater than 10^4 Hz in well consolidated rocks.

In this paper we show practical applications of the approach for different data sets. For the first time, numerical simulations are performed in order to better understand the phenomena of the triggering mechanisms and to verify the SBRC algorithms. Firstly, we give a brief theoretical

introduction into SBRC for homogeneous, anisotropic, poroelastic media. Then, we describe the concept of the SBRC approach for the 3-D mapping of hydraulic diffusivity. Therefore, an equation similar to the eikonal equation for seismic wavefronts is derived which serves as a basis for the inversion procedure. For further details we refer to previous publications and the WIT report 2000. We demonstrate the SBRC method on two case studies, including data from sedimentary environment. We show numerical methods to create synthetic microseismicity clouds for different types of media and the verification of the reconstruction algorithms.

A SUMMARY OF THE CONCEPT OF THE SBRC-METHOD

In the low-frequency limit of the Biot equations (Biot 1962) the pore-pressure perturbation p can be approximately described by the following differential equation of diffusion:

$$\frac{\partial p}{\partial t} = \frac{\partial}{\partial x_i}\left[D_{ij}\frac{\partial}{\partial x_j}p\right], \tag{1}$$

where D_{ij} are components of the tensor of the hydraulic diffusivity, x_j ($j = 1, 2, 3$) are the components of the radius vector from the injection point to an observation point in the medium and t is the time. Equation (1) corresponds to the second-type Biot wave (the slow P-wave) in the limit of the frequency extremely low in comparison with the global-flow critical frequency (Biot 1962).

Often, a pore pressure perturbation at the injection point can be roughly approximated by a step function (see e.g., Shapiro et al, 2000), which differs from zero till the time t_0 of a particular seismic event. The power spectrum of this signal has the dominant part in the frequency range below $2\pi/t_0$. Thus, the probability that this event was triggered by signal components from the frequency range $\omega \leq 2\pi/t_0$ is high. This probability for the low energetic higher frequency components is low. However, the propagation velocity of high-frequency components is higher than those of the low frequency components. Thus, to a given time t_0 it is probable that events will occur at distances, which are smaller than the travel distance of the slow-wave signal with the dominant frequency $2\pi/t_0$. The events are characterized by a significantly lower probability for larger distances. The spatial surface which separates these two spatial domains we call the triggering front.

Triggering fronts and scalar estimation of hydraulic diffusivity

In a first simple variant of the method, a homogeneous and isotropic medium is assumed. For a time-harmonic perturbation of the pore-pressure Shapiro et al. (1997) obtain the following equation describing the spatial position of the triggering front in an effective isotropic homogeneous poroelastic medium with the scalar hydraulic diffusivity D:

$$r = \sqrt{4\pi D t}. \tag{2}$$

Equation (2) provides scalar estimates of D only. For a homogeneously distributed diffusivity D_{ij}, the complete heterogeneous seismically-active rock volume is replaced by an effective homogeneous anisotropic poroelastic fluid-saturated medium. The permeability tensor of this effective medium is the permeability tensor of the heterogeneous rock upscaled to the characteristic size of the seismically-active region.

Inversion for the permeability

The tensor of the hydraulic diffusivity is just proportional to the tensor of the permeability. The coefficient A of this proportion is a poroelastic modulus divided by the fluid dynamic viscosity. In real rocks variations of the permeability are much larger than variations of the coefficient A. Thus, in order to estimate the permeability the most important step is to estimate D_{ij}. Then, in a good approximation, the diffusivity can be just scaled by a constant value of A estimated from e.g., log data (for more details see Shapiro et al, 1999 and 1997).

As we have seen above, the propagation of the triggering front is approximately defined by kinematic features of a slow-wave front of a particular frequency. For the SBRC approach, the earliest microseismic events are of importance. It is natural to assume that for their triggering in a heterogeneous medium a possibly quickest front configuration will be responsible. On the other hand, in the low-frequency range, the slow wave represents the process of the pore pressure relaxation and, therefore, is a diffuse wave. Recent observations on diffusive waves leads to the idea to use a geometrical-optics like description of triggering fronts to approximate the inversion procedure.

Considering relaxation of a harmonic component of a pressure perturbation of frequency ω, a standard eikonal equation can be derived describing the frequency-dependent phase travel time T in isotropic poroelastic media (see Shapiro et al., 2001):

$$|\nabla T|^2 = \frac{1}{2\omega D}. \tag{3}$$

The right hand part of this equation is the squared slowness of the slow wave.

Equation (3) is equivalent to the Fermat's principle which ensures the minimum time (stationary time) signal propagation between two points of the medium. Thus, it describes the minimum-time maximum-energy front configuration. In the case of an isotropic poroelastic medium equation (3) can be directly used to reconstruct a 3-D heterogeneous field of the hydraulic diffusivity. In the case of a step-function like pressure perturbation, from this an equation is derived which will describe the triggering time $t(\mathbf{r})$ (see Shapiro et al., 2001):

$$|\nabla t|^2 = \frac{t}{\pi D}. \tag{4}$$

Equation (4) will serve as a basis for the inversion procedure to reconstruct the spatial distributions of the hydraulic diffusivity in heterogeneous media.

CASE STUDIES

The SBRC-method was already successfully applied to several field examples and data from different types of reservoirs and injection experiments so far (see e.g. Shapiro et al. (1997, 1999, 2000); Rothert et al. (2001)). In the following, we want to show two examples of microseismicity data, which were created during a Hot-Dry-Rock experiment in crystalline rock and during a hydraulic fracturing experiment in sedimentary environment. The SBRC-algorithms are applied to reconstruct the maximum scalar value of hydraulic diffusivity/permeability as well as the 3D-distribution of it's magnitude within the seismically active rock volume on large spatial scales.

Figure 1(a) shows the spatio-temporal distribution of the microseismicity cloud collected in December 1983 during an injection experiment into crystalline rock at a depth of 3460 meters at the Fenton Hill (USA) geothermal energy site (for details and further references see Fehler et al., 1998). For each event the color denotes its occurrence time with respect to the start time of the injection.

If the value of the hydraulic diffusivity in equation (2) is selected correctly, then this equation will correspond to the upper bound of the cloud of events in the plot of their spatio-temporal distribution (i.e., the plot of r versus t). The scalar value of D is obtained by envelope fitting in the space-time domain. Figure 1(b) shows the estimation of the scalar hydraulic diffusivity for this data set. We observe good agreement between the theoretical curve with $D = 0.17 m^2/s$ and the data.

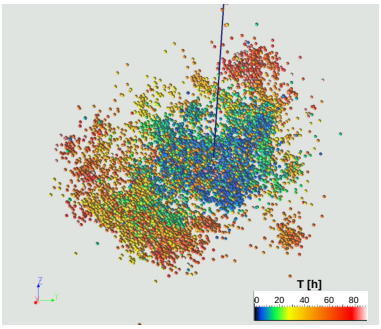

(a) Microseismicity cloud Fenton Hill

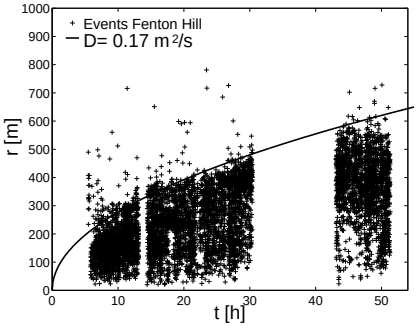

(b) Estimation of scalar hydraulic diffusivity

Figure 1: (a) The cloud of events from the 1983 injection experiment at Fenton Hill (USA) looking from the east. The color of the events corresponds to the event occurrence time. The injection took place at a depth of 3460m, the spatial extend shown is approx 1200m. The solid line indicates the borehole. (b) Estimation of the scalar hydraulic diffusivity at Fenton Hill yielding the maximum estimate $D_{max} = 0.17$ m^2/s.

Such good agreement supporting the concept of the triggering of microseismicity can be observed in many other cases. Figure 2(a) shows the spatio-temporal distribution of microseismic events observed during a hydrofracturing experiment in the Cotton Valley field, Panola country, East Texas (USA) in May 1997. Data was provided by courtesy of Ted Urbancic, Engineering Seismology Group Inc., Canada. About 994 events with high signal-to-noise ratio were localized during the injection in sedimentary environment up to 10h after the start of the injection (see Urbancic et al., (1999)). In Figure 2(b) the estimation of the scalar hydraulic diffusivity is shown. According to equation (2) the distance of each event is plotted versus its occurrence time after the beginning of the injection. The diffusivity $D = 0.36m^2/s$ was observed for the seismically-active volume at the depth of 2750-2850 meters by envelope fitting. Nevertheless, note again that these estimations only correspond to the maximum scalar value of hydraulic diffusivity for the entire seismically active rock volume and don't provide features like directions of increased hydraulic diffusivity.

Recently, a new algorithm was proposed for estimating the global tensor of hydraulic diffusivity. This algorithm is based on the transformation of the microseismicity cloud into a scaled coordinate system. Like for the scalar case one can obtain the tensor of hydraulic diffusivity by ellipsoidal fitting of the event cloud. With this estimation it is possible to study correlations of main axes of hydraulic diffusivities and e.g. main stress directions. For details, see Rindschwentner (2000) and Rindschwentner (2001).

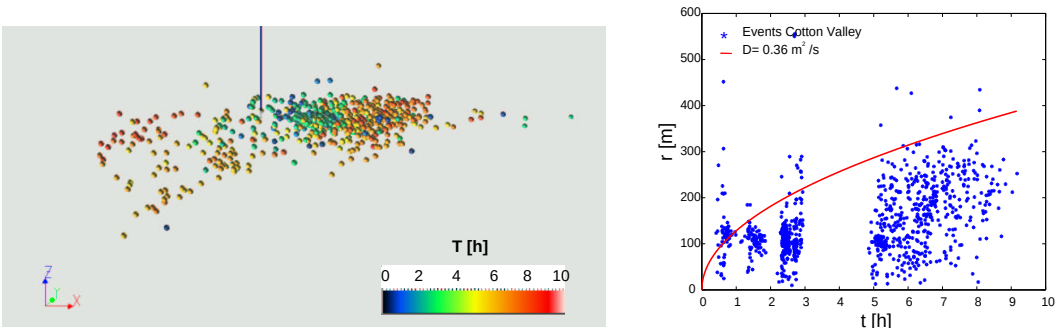

(a) Microseismicity cloud Cotton Valley

(b) Estimation of scalar hydraulic diffusivity

Figure 2: (a) The cloud of events from the 1997 injection experiment at the Cotton Valley site (USA) looking from the south. The color of the events corresponds to the event occurrence time. The injection took place at a depth of 2750-2850m, the spatial extend in x-direction is approx. 900m. The dark-blue line indicates the borehole. (b) Estimation of scalar hydraulic diffusivity at Cotton Valley yielding the estimate $D = 0.36$ m^2/s.

In order to show the practical application of the SBRC reconstruction algorithms for the 3D-distribution of hydraulic diffusivity, let us consider the aforementioned example of the mi-

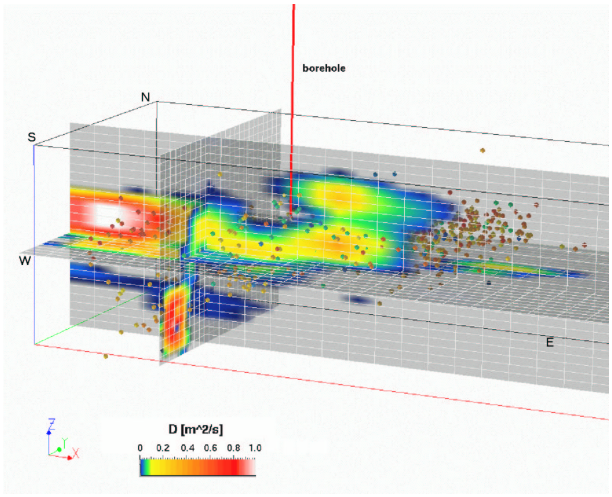

Figure 3: 3D-reconstruction of hydraulic diffusivity for Cotton Valley together with the microseismic events. Blue colors indicate low diffusivities, red colors indicate high values. The diffusivity ranges from 0.001 to 1 m^2/s. A high-permeable channel can be identified in the EW-direction (x-direction) from this data set.

croseismicity cloud collected during the hydrofracturing experiment at the Cotton Valley test site in May 1997 (see Urbancic al., 1999). If the space of the seismically active rock volume (Fig. 2(a)) is subdivided into a number of 3D cells, an arrival time of the triggering front can be defined into each cell. Of course, some smoothing is required. Such a surface can be constructed for any arrival time presented in microseismic data. Thus, the time evolution of the triggering surface, i.e., the triggering front propagation can be characterized. In a heterogeneous porous medium, the propagation of the triggering front is determined by its heterogeneously distributed velocity. Given the triggering front positions for different arrival times, the 3-D distribution of the propagation velocity can be reconstructed. In turn, the hydraulic diffusivity is directly related to this velocity.

Figure 3 shows the 3D-reconstruction of hydraulic diffusivity for the Cotton Valley data set. For the inversion, the isotropic variant of the method was used. A permeable channel can clearly be identified in the EW-direction from the borehole (yellow and red zones in Fig. 3).

NUMERICAL SIMULATIONS OF THE TRIGGERING PHENOMENON

In order to better understand the phenomenon of the triggering process due to pore pressure perturbation, numerical experiments are performed. For the first time, it is thereby possible to test the SBRC algorithms with synthetic data. Methods were developed making it possible to study influences of different media types on the spatio-temporal behavior of induced seismicity clouds.

Using a finite element algorithm (FE) and the MATLAB® computing environment, the time-

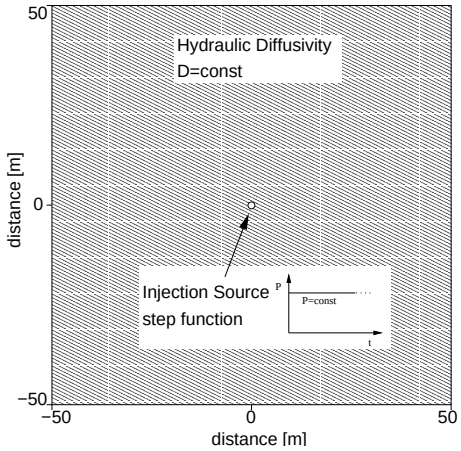

Figure 4: Sketch of a simple model used for numerical tests. The dimensions of the 2D-model are 100×100 m, the scalar diffusivity is distributed homogeneously in the medium. The source point of injection is located in the center of the box with a step-function like perturbation of the pressure. The duration of the injection is 100 seconds for which the time-dependent equation of diffusion is solved to obtain the pressure perturbation within the model.

dependent parabolic equation of diffusion for a 2D homogeneous, isotropic background medium is solved. The source point is located in the center of a model. As input signal a step-function like pressure perturbation with constant amplitude is used. A sketch of the model is shown in Figure 4. After obtaining the time-dependent pressure perturbation within the model for the modeling duration of 100 seconds, the medium is divided into small cells. A failure-criterion (trigger-criterion) is then randomly distributed. This procedure directly follows the concept of the SBRC-method, that real rocks are in a subcritical state of stress in some randomly distributed places. Triggering of microseismicity occurs in places, where the amplitude of pore pressure perturbation exceeds the failure criterion. The graphical user interface (GUI) together with an example for the distribution of the triggering-criterion is shown in Figure 5.

For each time step and within each cell the pressure variation (obtained by the solution of the diffusion equation) is compared with the trigger-criterion. If the value of the failure-criterion within one cell is exceeded by the pressure variation, an event triggered at this point is defined. With this procedure we are able to create synthetic microseismicity clouds and to model the spatio-temporal evolution of the events. Additionally we are able to study the influence of different types of the medium statistics on the triggering process. For this purpose it is possible to correlate the failure-criterion spatially by including autocorrelation functions, e.g. like gaussian or exponential. An example for gauss-correlated distributions of the trigger-criterion with different correlation-distances is shown in Figure 6. Note, that of course we are not able to include effects like reinforcement of the triggering effect due to self-induction so far, i.e. induced pore pressure perturbation due to the release of an event itself.

Figure 7 shows the result of the numerical modeling procedure. The synthetic clouds of

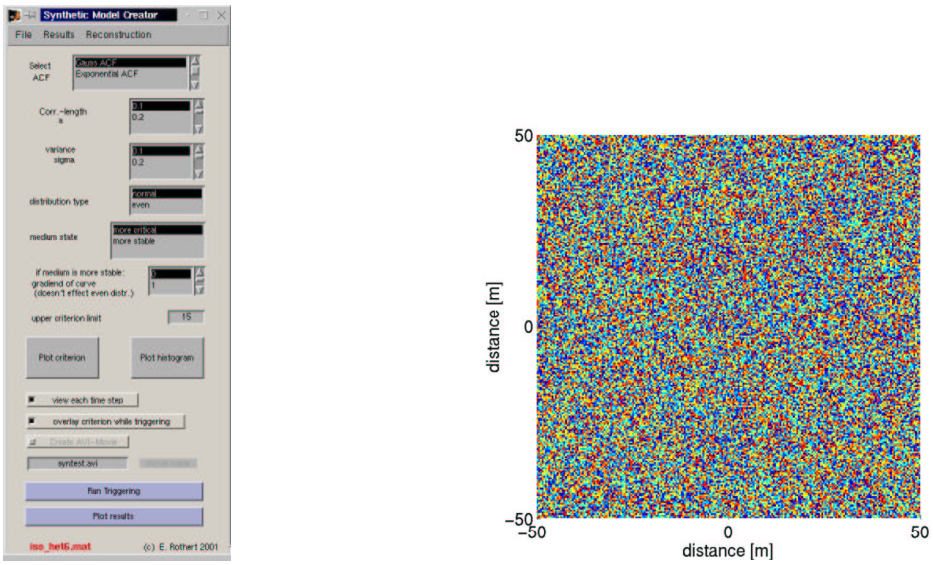

(a) Graphical user interface (GUI)

(b) Distribution of failure criterion

Figure 5: Graphical user interface for performing numerical experiments (a). It is used to create different distributions of the triggering criterion in the model. (b) Example for the distribution of the failure criterion. Within each cell a random value of critical pore pressure is calculated which - once exceeded - results in the triggering of a microseismic event. The color denotes the value of the failure-criterion, blue colors correspond to zones where the medium is highly critical, red colors denote a stable and unbreakable medium.

events generated after 100s of modeling using the distribution of the failure-criterion in Figure 6(a) and 5(b) are shown, respectively. In Figure 8 the estimation of the scalar hydraulic diffusivity using equation (2) is shown for the data set of Figure 7(b). It is obvious, that the observed spatio-temporal distribution of the events agrees very well with the predicted behavior. The preset value of diffusivity used in the homogeneous model ($D = 1\,\mathrm{m}^2/\mathrm{s}$) is reconstructed quite well which is shown by the red line of the envelope function. Note again, that the envelope fit only corresponds to the upper limit of the hydraulic diffusivity in the medium.

Heterogeneous model and reconstruction of diffusivity

The numerical modeling procedure does not only allow to study the triggering phenomenon within homogeneous and isotropic media, it also provides the possibility to include any desired type of background model. Media with heterogeneously distributed hydraulic diffusivity can be treated as well as anisotropic ones. An example for a simple heterogeneous model is shown in Figure 9(a). Here, two values of scalar diffusivity are used. The cross-shape structure is characterized by an increased value of diffusivity ($D_1 = 50\mathrm{m}^2/\mathrm{s}$), whereas its value in the border

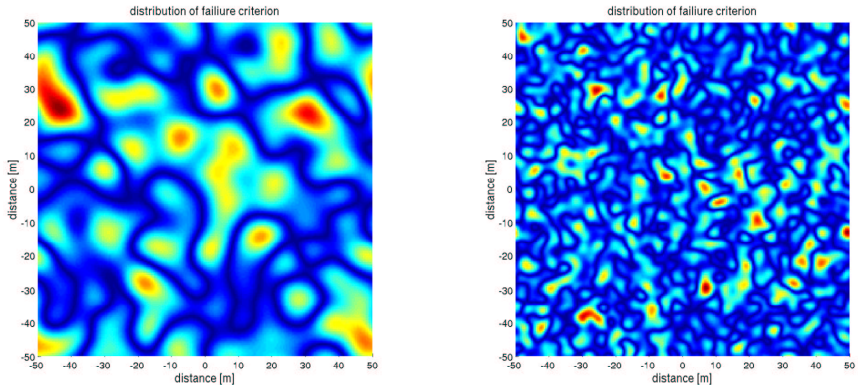

(a) **(b)**

Figure 6: Examples for the distribution of the spatially correlated triggering criterion with gaussian function for two different correlation distances. It is possible to include structures like failure-zones in the medium and to study the effects of different medium statistics on the triggering of microseismicity. The color corresponds to the criticality of the medium, blue zones denotes small values of the failure-criterion (highly critical), red colors show stable zones within the medium.

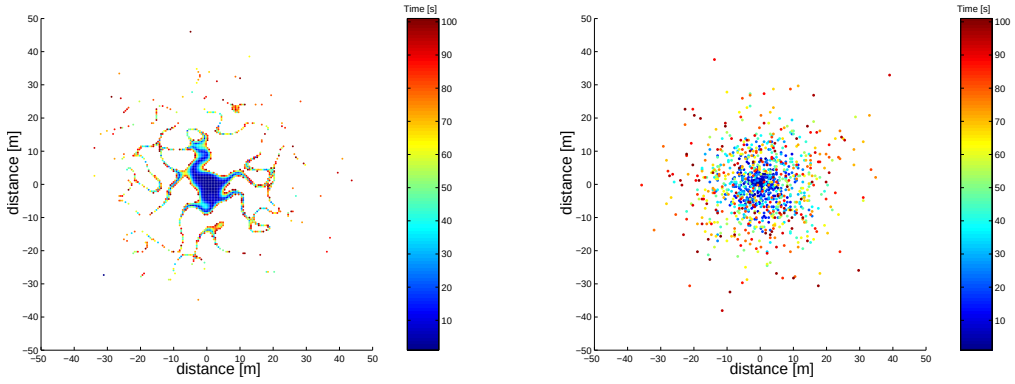

(a) **(b)**

Figure 7: Synthetic event clouds after modeling using the distribution of the failure-criterion of Figure 6(a) and 5(b), respectively. The color denotes the event occurrence time. For model (a) a total number of 1984 events were generated, model (b) results in 2636 events triggered.

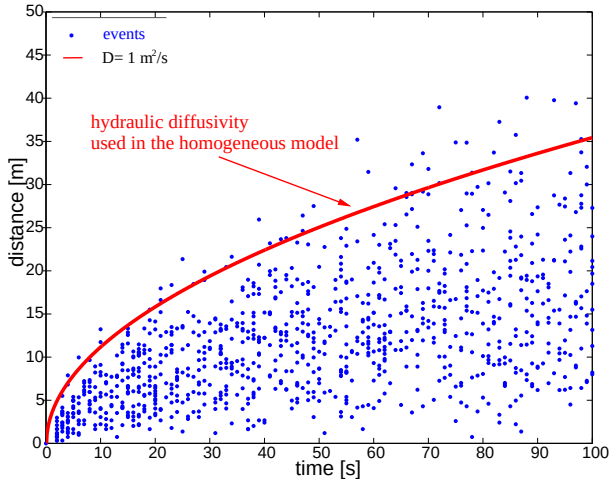

Figure 8: Estimation of the scalar hydraulic diffusivity for the event cloud (Figure 7(b) generated by numerical modeling. The solid line corresponds to the predicted value of diffusivity used in the homogeneous background model. 95.7 % of all events triggered are located below the envelope function in the space-time-domain.

regions is 10 times smaller ($D_2 = 5\text{m}^2/\text{s}$). The purpose of the modeling is first to study the spatio-temporal evolution of events triggered, second the verification of the approach to reconstruct the maximum scalar value of diffusivity and lastly the reconstruction of the structure of the medium by application of the SBRC-algorithms. The amplitude of pressure perturbation after the modeling time of 100 seconds together with isolines is shown in Figure 9(b). As input signal a step-function like pressure perturbation with constant amplitude in the center of the model is used.

The result of the triggering process is shown in Figure 10(a). The value of hydraulic diffusivity in the model as well as the distribution of the trigger-criterion was chosen in such a way to fill out the whole model with events. This is an important factor, because the SBRC-method only can reconstruct diffusivity in regions where the statistics of events is large enough, i.e. preferably large amount of events in the cells used for reconstruction. A total amount of 20337 events were triggered during the modeling procedure. The estimation of scalar hydraulic diffusivity from this data set is shown in Figure 10(b). The coordinates of the events in the space-time domain are shown as blue dots, the red solid lines represent the two values of hydraulic diffusivity used in the model according to equation (2), respectively. It is obvious, that even for this model the spatio-temporal structure of the events fulfill the predicted behavior. 99.91 % of all events are located below the envelope-function with $D = D_{max} = 50\text{m}^2/\text{s}$. Thus, the SBRC-algorithms for estimation of scalar hydraulic diffusivity even works quite well for heterogeneous media. Even for anisotropic models (not shown here) the reconstruction of maximum value of diffusivity works well.

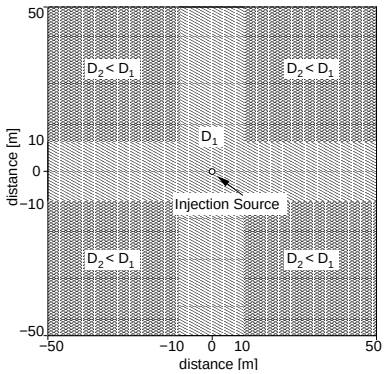

(a) Heterogeneous model

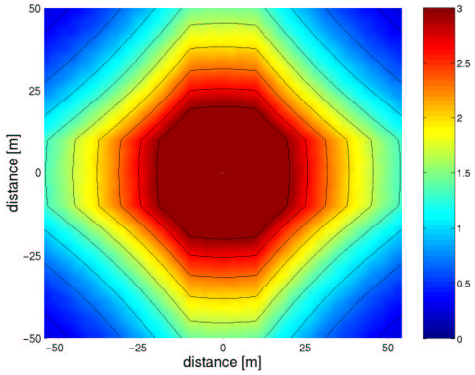

(b) Solution of diffusion equation with isolines

Figure 9: Sketch of a heterogeneous model used for numerical experiments (a) and solution of the diffusion equation after 100 seconds of modeling (b). The color denotes the amplitude of pressure perturbation, isolines are shown for constant amplitudes as black lines.

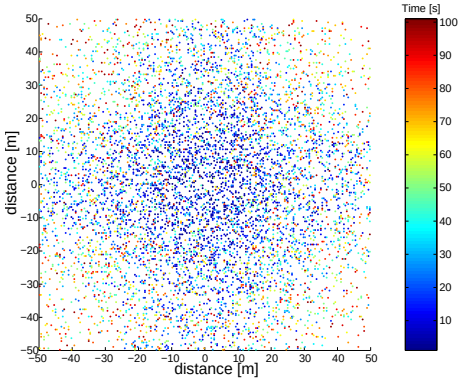

(a) Event cloud heterogeneous model

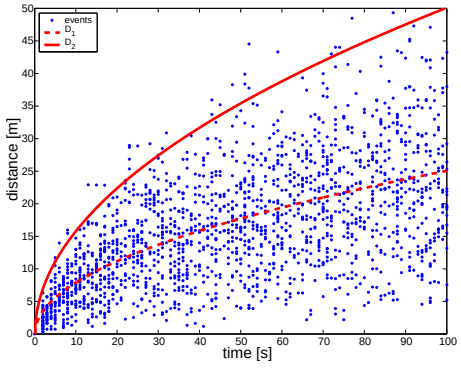

(b) Estimation of scalar hydraulic diffusivity

Figure 10: (a) Cloud of events and its distribution in heterogenous model. The color denotes the event occurrence time up to 100 seconds of modeling. Figure (b) shows the estimation of scalar hydraulic diffusivity from this data set.

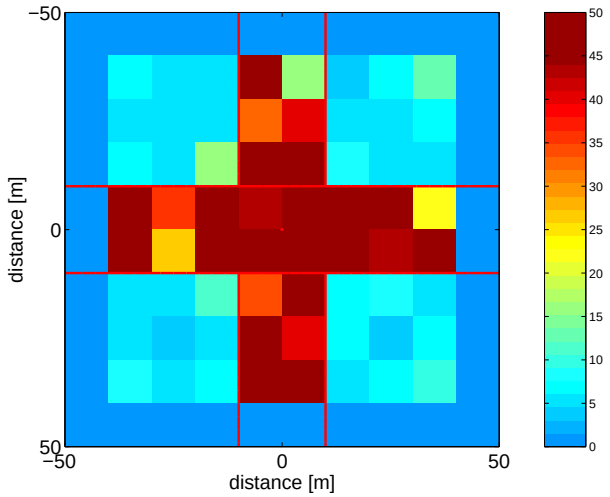

Figure 11: Reconstruction of diffusivity distribution in the heterogeneous model. The color denotes the amplitude of diffusivity. The geometry used in the model (indicated by the red lines) is reconstructed quite well.

In order to reconstruct the distribution of hydraulic diffusivity in 2D, the SBRC-algorithms on the basis of equation (3) are applied. The model is subdivided into 10×10 cells each containing approx. 475 potential events. Thus, the statistical requirements for the algorithm is fulfilled. The result of the inversion procedure is shown in Figure 11. It is obvious, that the overall structure (cross-shape) of the medium is reconstructed quite well. However, problems occur due to failures calculating of the time derivatives in the border regions.

CONCLUSIONS

We have shown the application of the SBRC approach for reconstructing the diffusivity/permeability distribution in 3-D heterogeneous poroelastic media using microseismicity induced by a borehole-fluid injection. Results of this inversion for hydraulic properties of reservoirs can be used at least semi-quantitatively to characterize geothermal as well as hydrocarbon reservoirs. They can be extremely helpful as constrains to reservoir simulations. In addition, we have proposed an approach to model the triggering phenomenon numerically. These numerical experiments support the SBRC. Moreover, they can be used to study the influence of different statistics of media on the triggering-phenomenon of events due to pore pressure relaxation.

REFERENCES

Biot, M. A. (1962). Mechanics of deformation and acoustic propagation in porous media. *Journal of Applied Physics*, 33:1482–1498.

Cornet, F. H. (2000). Comment on 'large-scale *in situ* permeability tensor of rocks from in-

duced microseismicity' by S.A. Shapiro, P. Audigane and J.-J. Royer. *Geophysical Journal International*, 140:465–469.

Fehler, M., House, L., Phillips, W. S., and Potter, R. (1998). A method to allow temporal variation of velocity in travel-time tomography using microearthquakes induced during hydraulic fracturing. *Tectonophysics*, 289:189–202.

Rindschwentner, J. (2000). Estimating the Global Permeability Tensor using Hydraulically Induced Microseismicity - Implementation of a new Algorithm. *WIT Report 2000*, pages 145–157.

Rindschwentner, J. (2001). Estimating the global permeability tensor using hydraulically induced seismicity - implementation of a new algorithm and case studies. Master thesis, 101 pages, Freie Universität Berlin.

Rothert, E., Shapiro, S. A., and Urbancic, T. (2001). Microseismic reservoir characterization: numerical experiments and cas studies. In *Expanded Abstracts*, San Antonio. 71st SEG Meeting.

Shapiro, S. A., Audigane, P., and Royer, J.-J. (1999). Large-scale in situ permeability tensor of rocks from induced microseismicity. *Geophysical Journal International*, 137:207–213.

Shapiro, S. A., Huenges, E., and Borm, G. (1997). Estimating the crust permeability from fluid-injection-induced seismic emission at the KTB site. *Geophysical Journal International*, 131:F15–F18. (see also Corrigendum, Geoph. J. Int., 1998, v.134, p.913).

Shapiro, S. A., Rothert, E., Rath, V., and Rindschwentner, J. (2001). Characterization of fluid transport properties of reservoirs using induced microseismicity. *Geophysics*, accepted.

Shapiro, S. A., Royer, J.-J., and Audigane, P. (2000). Reply to comment by F.H. Cornet on 'large-scale in situ permeability tensor of rocks from induced microseismicity'. *Geophysical Journal International*, 140:470–473.

Urbancic, T. I., Shumila, V., Rudledge, J. T., and Zinno, R. J. (June 6-9, 1999). Determining hydraulic fracture behavior using microseismicity. *Vail Rocks '99, 37th U.S. Rock Mechanics Symposium, Vail, Colorado*.